NeuroImage: Clinical 4 (2014) 488–499

Contents lists available at ScienceDirect

NeuroImage: Clinical

journal homepage: www.elsevier.com/locate/ynicl

Altered resting-state functional connectivity in patients with chronic bilateral vestibular failure

Martin Göttlich, Nico M. Jandl, Jann F. Wojak, Andreas Sprenger, Janina von der Gablentz, Thomas F. Münte, Ulrike M. Krämer, Christoph Helmchen*

Department of Neurology, University of Lübeck, Ratzeburger Allee 160, Lübeck 23538, Germany

ARTICLE INFO

Article history:
Received 15 January 2014
Received in revised form 26 February 2014
Accepted 9 March 2014

Keywords:
Resting-state fMRI
Functional connectivity
Degree
Bilateral vestibular failure
Vestibulo-ocular reflex

ABSTRACT

Patients with bilateral vestibular failure (BVF) suffer from gait unsteadiness, oscillopsia and impaired spatial orientation. Brain imaging studies applying caloric irrigation to patients with BVF have shown altered neural activity of cortical visual–vestibular interaction: decreased bilateral neural activity in the posterior insula and parietal operculum and decreased deactivations in the visual cortex. It is unknown how this affects functional connectivity in the resting brain and how changes in connectivity are related to vestibular impairment.

We applied a novel data driven approach based on graph theory to investigate altered whole-brain resting-state functional connectivity in BVF patients (n= 22) compared to age- and gender-matched healthy controls (n= 25) using resting-state fMRI. Changes in functional connectivity were related to subjective (vestibular scores) and objective functional parameters of vestibular impairment, specifically, the adaptive changes during active (self-guided) and passive (investigator driven) head impulse test (HIT) which reflects the integrity of the vestibulo-ocular reflex (VOR).

BVF patients showed lower bilateral connectivity in the posterior insula and parietal operculum but higher connectivity in the posterior cerebellum compared to controls. Seed-based analysis revealed stronger connectivity from the right posterior insula to the precuneus, anterior insula, anterior cingulate cortex and the middle frontal gyrus. Excitingly, functional connectivity in the supramarginal gyrus (SMG) of the inferior parietal lobe and posterior cerebellum correlated with the increase of VOR gain during active as compared to passive HIT, i.e., the larger the adaptive VOR changes the larger was the increase in regional functional connectivity.

Using whole brain resting-state connectivity analysis in BVF patients we show that enduring bilateral deficient or missing vestibular input leads to changes in resting-state connectivity of the brain. These changes in the resting brain are robust and task-independent as they were found in the absence of sensory stimulation and without a region-related a priori hypothesis. Therefore they may indicate a fundamental disease-related change in the resting brain. They may account for the patients' persistent deficits in visuo-spatial attention, spatial orientation and unsteadiness. The relation of increasing connectivity in the inferior parietal lobe, specifically SMG, to improvement of VOR during active head movements reflects cortical plasticity in BVF and may play a clinical role in vestibular rehabilitation.

1. Introduction

Bilateral vestibular failure (BVF) is a severe chronic disorder of the labyrinth or the eighth cranial nerve characterized by unsteadiness of gait and oscillopsia during head movements (Brandt, 1996). BVF has a wide spectrum of etiologies (Zingler et al., 2007). The most common cause of BVF is vestibulotoxicity of ototoxic drugs (specifically aminoglycosides). New technical improvements allowing precise and easy assessment of vestibular function by videooculography have shown that BVF is much more common as previously believed but etiology often remains unknown, i.e., idiopathic BVF (Machner et al., 2013). Clinical signs and prognosis of BVF are different from those of unilateral vestibular failure (UVF). Vestibular neuritis patients complain about acute vertigo and show spontaneous nystagmus and lateropulsion in the acute phase. They have a fairly good recovery although a third of all patients do not show peripheral regeneration. This has partly been attributed to cortical and subcortical mechanisms of compensation which have been studied by various brain imaging techniques, using PET (Becker-Bense et al., 2013; Bense et al., 2004a), voxel based morphometry (Helmchen et al., 2009; Helmchen et al., 2011; Zu Eulenburg et al., 2010) and functional imaging of resting-state connectivity

* Corresponding author.
E-mail address: christoph.helmchen@neuro.uni-luebeck.de (C. Helmchen).

http://dx.doi.org/10.1016/j.nicl.2014.03.003

(Helmchen et al., 2013).

The characteristic symptoms of BVF patients, oscillopsia and blurred vision during head movements and locomotion, result from a deficient vestibulo-ocular reflex (VOR) which normally stabilizes gaze during rapid head movements. Gait unsteadiness in BVF is often not attributed to a deficient VOR and therefore misdiagnosed. Unfortunately, about 80% of BVF patients do not recover which may be due to brain mechanisms which are entirely different from UVF (Dieterich and Brandt, 2008a). While partial or complete peripheral vestibular nerve regeneration (Palla and Straumann, 2004; Schmid-Priscoveanu et al., 2001) and central, presumably compensatory, mechanisms contribute to vestibular rehabilitation in vestibular neuritis (Alessandrini et al., 2009; Becker-Bense et al., 2013; Bense et al., 2004a; Helmchen et al., 2009; Helmchen et al., 2013; Zu Eulenburg et al., 2010) peripheral nerve dysfunction and dizziness in BVF are often permanent (Zingler et al., 2008). As the contralesional vestibular input subserving cortical vestibular processing is missing, other non-vestibular mechanisms have been suggested to provide central vestibular compensation in BVF, e.g., substitution by changing the gain in the somatosensory (Strupp et al., 1998) or visual system (Dieterich et al., 2007a). Recently, a possibly adaptive mechanism of enhanced proprioceptive signal interaction with cortical visual processing has been found in BVF patients presumably subserving proprioceptive substitution of vestibular function (Cutfield et al., 2014).

In a recent meta-analysis considering 28 PET and fMRI studies employing vestibular stimuli to healthy subjects Zu Eulenburg et al. (2012) suggested the cytoarchitectonic area OP2 (Eickhoff et al., 2005) in the parietal operculum as the primary candidate for the human vestibular cortex. In patients with BVF, PET brain imaging ($H_2{}^{15}O$) during vestibular caloric stimulation revealed decreased bilateral activation in the "parieto-insular vestibular cortex" (PIVC) compared to healthy controls (Bense et al., 2004b). Intersensory cortical processing, specifically reciprocal cortical inhibitory visual–vestibular interaction seemed to be preserved, though at reduced levels, i.e., bilateral deactivation of the visual cortex, which is normally encountered during vestibular stimulation in healthy subjects, was reduced and the posterior insula was less activated bilaterally in BVF patients (Bense et al., 2004b). These data are based on behavioral or event-related brain activation studies. Changes in event-related activation studies can be ambiguous as they may not reflect the underlying pathophysiological mechanisms but only their behavioral consequences. In contrast, looking at the brain's activity at rest (resting-state) might shed more light on fundamental changes of functional connectivity in the brain. Due to the lack of task demands, resting-state fMRI (RS-fMRI) does not require an experimental design, patient's compliance, and training, making it attractive in a clinical environment. However, none of the previous studies looked at resting-state brain activity in BVF patients using fMRI.

Recently, using RS-fMRI, we have shown decreased functional connectivity in the intraparietal sulcus and supramarginal gyrus of patients with unilateral vestibular neuritis which partially reversed over a period of three months when patients had improved. Interestingly, this increase tended to be larger in patients with only little disability in the follow-up examination suggesting a role in vestibular compensation (Helmchen et al., 2013).

In this study we examined brain intrinsic functional connectivity in patients with bilateral vestibular failure (BVF). We used a novel data driven approach based on graph theory to investigate altered whole brain intrinsic functional connectivity in BVF patients as compared to healthy controls. The so-called degree centrality (Bullmore and Sporns, 2009) served as a marker for altered connectivity. In graph theory, the degree of a vertex (node) is defined as the number of links (edges) connected to the node. The degree is thus a measure for the connectedness of a node within a network. Here, voxels serve as nodes and edges are defined by the functional connectivity between voxels. In contrast to network analyses which depend on a given parcellation of the brain, this approach has a higher spatial resolution and is not biased by a priori defined anatomical structures. In previous studies, voxel-based network analyses were performed to investigate topological properties of the brain network (van den Heuvel et al., 2008) and to identify network hubs, i.e., brain regions which show a strong connectivity to the rest of the brain (Buckner et al., 2009; Zuo et al., 2012). Recently, the voxel-degree method was successfully used as a marker for altered resting state functional connectivity in Alzheimer's disease (Buckner et al., 2009), Parkinson's disease (Göttlich et al., 2013), and Obsessive Compulsive Disorder (Beucke et al., 2013).

The aim of our study on BVF patients was therefore to elucidate (i) whether there are changes in functional connectivity in brain areas involved in processing of vestibular information and (ii) whether these changes during resting-state are related to subjective or objective parameters of vestibular impairment. Specifically, we chose the deficient gain of the VOR which can be improved in a behavioral context: UVF patients increase their VOR gain during self-guided, active and thereby predictive head impulse movements as compared to non-predictive, passive head impulses (Black et al., 2005; Sprenger et al., 2006). We hypothesized that BVF patients are also capable of using non-vestibular predictive mechanisms to stabilize images of the visual world on the fovea. Therefore we compared functional connectivity within neural networks in BVF patients with age- and gender matched healthy controls and related the differences in this (active vs. passive) vestibulo-ocular behavior to changes in functional connectivity.

2. Materials and methods

2.1. Participants

Patients with bilateral vestibular failure (BVF) were compared with age and gender matched healthy control subjects. The study was approved by the institutional ethics committee of the University of Lübeck. All participants gave written informed consent before their inclusion into the study. The study was performed in agreement with the Declaration of Helsinki. Participants were recruited from an outpatient neurology clinic in a tertiary care academic medical center at the University of Lübeck (Dizziness Center in Lübeck, Germany). Patients complained about dizziness, gait unsteadiness and oscillopsia during locomotion and head movements. All participants were right-handed and underwent extensive neurologic, neuro-ophthalmologic, and neuro-otologic examinations. BVF patients were on no regular medication known to affect central nervous system processing. None of the patients took any antivertiginous medication during the examination day. Patients were diagnosed to have BVF based on clinical examinations by experienced neurologists and neuro-otologist of the University Dizziness Center in Lübeck and electrophysiological recordings [bithermal cold (27°) and warm (44°) caloric irrigation, quantitative head impulse test] were analyzed by a co-worker with longstanding experience in assessing vestibular function by caloric and quantitative head impulse videooculography who did not know about the history and clinical findings of the patients. Inclusion criteria for BVF were the following: (1) clinical assessment of a bilaterally pathologic HIT (Jorns-Haderli et al., 2007), (2) bilaterally reduced gain of the horizontal VOR (<0.72) assessed by video-HIT (Machner et al., 2013) (3) bilateral caloric hyporesponsiveness (mean peak slow phase velocity (SPV) of $<5°/s$ on both sides), and (4) cranial magnetic resonance imaging without structural brain lesions. Patients with depression (as assessed by the Beck depression score) and dementia (assessed by the MOCA scale) and those with additional evidence of autoimmune and paraneoplastic diseases were excluded from the study. Participants subjectively rated their level of disease-related impairment by the Vertigo Handicap Questionnaire (VHQ) (Tschan et al.,

2010), the Vertigo Symptom Scale (VSS) (Tschan et al., 2008), the Clinical Vestibular Score (CVS) (Helmchen et al., 2009), and the Subjective Dizziness Score (SDS) (Helmchen et al., 2009). A total number of 33 patients with chronic (>3 months, range: 3 months to 20 years) BVF were examined. 11 patients had to be excluded for various reasons: extensive head motion during MRI recordings (n= 6), comorbidity (n= 3) and brain lesions on MRI examinations (n= 2). This resulted in 22 eligible BVF patients (12 males; age: 65.6 ± 9.8 years; disease duration: range 3 months to 20 years). The most common etiology of BVF was antibiotic ototoxicity (n = 13; 59%), followed by idiopathic BVF (n = 4; 18%), sequential vestibular neuritis (n = 2; 9%), cerebellar ataxia with BVF (n= 2; 9%) and Meniere's disease (n = 1; 5%). Thirty healthy control subjects were recruited. All participants had normal structural MR images showing no signs of cerebral atrophy. Three control subjects were excluded due to extensive head motion and two subjects due to neuropsychiatric symptoms. Twenty-five healthy control subjects (14 males; age: 65.0 ± 9.2 years) were included in the study. The patient and the control group did not differ significantly in age (two-sample t-test p = 0.81; degrees of freedom: 45) or gender (chi-square test p = 0.71).

All participants were examined by a battery of vestibular investigations. Semicircular canal function was investigated by electronystagmography with caloric irrigation and quantitative head impulse test (qHIT) and otolith function by static (background stationary) and dynamic (moving visual background) subjective visual vertical (SVV) (Dieterich and Brandt, 1993) and vestibular evoked myogenic potentials (VEMPs). Psychophysical perception of the visual vertical was assessed by the subject's adjustment of a bar to the perceived visual vertical without any spatial orientation clues in a dotted hemispherical dome, which is stationary or moving around the line of sight (Dieterich and Brandt, 1993). The normal range of SVV was defined as deviation of <2.5°. Several but not all patients and all healthy participants were investigated by ocular and cervical vestibular evoked myogenic potentials (oVEMP, cVEMP) (Curthoys et al., 2012; Rosengren and Kingma, 2013). We used a vibration stimulus at the mid-forehead delivered by a minishaker (Brüel & Kjaer, Denmark) to elicit oVEMPs recorded from surface EMG electrodes beneath the lower orbital rim above the obliquus inferior muscle. To activate this muscle subjects fixated a target above their forehead. oVEMP was taken at a latency of about 10 ms from the stimulus-locked ocular vestibular-evoked myogenic potential and the first negative component. Cervical VEMPs were delivered by short tone bursts of 500 Hz to either ear (headphone) and recorded over tensed sternocleidomastoid (SCM) muscles bilaterally. This results in a stimulus-locked short-latency myogenic potential recorded (cVEMP) with an initial positive (inhibitory) potential (p13) followed by a negative potential (n23) (Rosengren et al., 2010).

2.2. Quantitative head impulse test

All participants were examined by quantitative head impulse test (qHIT) using video-oculography. Eye and head movements were recorded by the EyeSeeCam® HIT System (Autronics, Hamburg, Germany) at a sampling rate of 220 Hz. VOR gain was determined by robust linear regression of eye and head velocity starting at head velocity >10 °/s to 95% of peak head velocity using Matlab®. Quantitative HIT was delivered by passive head impulses (HIT) with rapid small amplitude (10–15°) horizontal head rotations (3000–4500°/s^2) while the participant was sitting on a chair fixating a red LED at a distance of 100 cm. Quantitative horizontal HIT was performed under the following conditions: Head impulses were either (i) passively conducted being unpredictable for direction and onset (inter-pulse interval: 4–6 s, passive condition) (Sprenger et al., 2006) or (ii) self-generated, i.e., actively performed (participant driven). Prior to the second condition (active HIT), participants learned to make active head-impulses in the same manner and velocity range as during passive head-impulses while staring at the LED. The investigator monitored peak head velocity during the active condition. We investigated if the VOR gain difference under active (participant driven) and passive (investigator driven) conditions is related to changes in functional connectivity.

2.3. Experimental design

The functional MRI data was acquired during a so-called resting-state block of 6 minute duration. Subjects were instructed not to engage in any particular cognitive or motor activity and to keep their eyes closed.

2.4. Image acquisition

Structural and functional MRI images were recorded on a Philips Achieva 3-T scanner (Philips Healthcare, the Netherlands). A total of N = 178 functional images were acquired using a T2*-weighted single-shot gradient-echo echo-planar imaging (EPI) sequence sensitive to blood oxygen level dependent (BOLD) contrast using the following parameters: repetition time TR = 2000 ms; echo time TE = 30 ms; isotropic 3 mm voxel size; field of view 192 mm; 34 slices; 0.75 mm interslice gap and flip angle 80°. The slices were recorded in ascending interleaved order starting with odd slices. A standard 8-channel phase array head coil was used. High resolution structural images were obtained applying a T1-weighted 3D turbo gradient-echo sequence with SENSE (image matrix 240 × 240; 180 slices; 1 × 1 × 1 mm^3 spatial resolution).

2.5. Preprocessing

Preprocessing was performed using the SPM8 software package (University College, London, Wellcome Trust Centre for Neuroimaging, *http://www.fil.ion.ucl.ac.uk/spm/*). The first 10 images of each dataset were discarded to allow for magnetization equilibrium and for the subjects to adjust to the environment. The preprocessing included the following steps: (i) Correction for differences in the image acquisition time between slices; (ii) a six parameter rigid body spatial transformation to correct for head motion during data acquisition; (iii) co-registration of the structural image to the mean functional image; (iv) gray and white matter segmentation, bias correction and spatial normalization of the structural image to a standard template (Montreal Neurological Institute); (v) in order to reduce the influence of motion and unspecific physiological effects, a regression of nuisance variables from the data was performed. Nuisance variables included white matter and ventricular signals and the six motion parameters determined in the realignment procedure; (vi) spatial normalization of the functional images using the normalization parameters estimated in the previous preprocessing step and resampling to 3 × 3 × 3 mm^3; (vii) spatial smoothing with a 6 mm full width half maximum Gaussian kernel; and (viii) a temporal bandpass filter was applied to all voxel time series (0.01 Hz < f < 0.08 Hz).

The six realignment parameters, i.e., three displacements and three elementary rotations with respect to the first image in the EPI series, were used as an estimator for the head motion. The displacements with respect to the first image of the series were required to be smaller than 3.0 mm (minimum to maximum) and the individual rotations smaller than 3.0°. Subjects showing any displacement or rotation greater than these cut-offs were excluded.

2.6. Voxel degree maps

Voxel degree maps were calculated by correlating the temporal BOLD signal fluctuation of each voxel with all other voxels in the brain and counting the number of connections above a certain threshold. As a measure for the temporal correlation, we computed the zero-lag Pearson's linear correlation coefficient r. The individual correlation

coefficients were entered into an $N \times N$ adjacency matrix where N is the number of voxels. The voxel network matrix was thresholded by $r > 0.25$ suppressing random correlations. This results in a binary undirected network matrix d_{ij}. The voxel degree D_i was derived from the network matrix as follows:

$$D_i = \sum_{j=1}^{N} d_{ij}.$$

The degree maps were z-transformed to allow for averaging and between subject comparisons:

$$z_i = \frac{D_i - \overline{D}}{\sigma_D} \, (i = 1 \ldots N).$$

Here, $\overline{D}$ denotes the mean degree and σ_D the standard deviation.

2.7. Seed-based functional connectivity

Seed-based connectivity analyses were performed to investigate the functional connectivity of a brain region of interest to the whole brain (Biswal et al., 1995; Vincent et al., 2006). The time courses of all voxels within a sphere of 6 mm radius around the center coordinate of a particular ROI were averaged and connectivity maps were calculated by correlating the mean time course to all voxel time courses within a brain mask. Correlations were computed using the Pearson product moment formula. A Fisher z-transform was applied to all correlation maps prior to the statistical analysis. A two-sample t-test was carried out to identify regions of altered connectivity.

2.8. Statistical analysis

Differences in the voxel degree between healthy controls and patients were investigated by a random effects analysis applying a two-sample t-test. Statistical images were assessed for cluster-wise significance using a cluster-defining threshold of $p = 0.005$. A topological false discovery rate (FDR) procedure was used to correct for multiple comparisons (Chumbley et al., 2010; Chumbley and Friston, 2009). The FDR-corrected critical cluster size was $k = 74$. Voxel-wise regression analyses were used to relate changes in regional connectivity with behavioral data. The analysis was performed using SPM8 (*http://www.fil.ion.ucl.ac.uk/spm/*). The statistical analysis of behavioral data was performed using Matlab®. If not stated otherwise we report the mean and standard deviation of the data.

3. Results

3.1. Behavioral data

The mean VOR gain was larger for the active compared to the passive HIT. The increase of VOR gain during active HIT (gain: 0.46 ± 0.24; $T(21) = 4.77$; $p < 0.0001$; Fig. 1C) was almost twofold as high compared to the passive HIT (VOR gain: 0.26 ± 0.18). An example of this VOR gain difference is shown in Fig. 1 with original eye and head velocity traces of passive (A) and active (B) head impulse test for a single patient.

oVEMPs were recorded in 22 patients and 23 healthy control subjects; they were absent in 12 patients and revealed reduced amplitudes in the other 10 patients: peak amplitude differed significantly between groups (Mann–Whitney U-Test $p = 0.003$, median patients: 3.8 μV, median healthy control subjects: 6.95 μV). cVEMPs were recorded in 22 patients and 23 healthy control subjects (median: 24.4 μV); they were absent in 17 patients and showed significantly reduced amplitudes in the other 5 patients (median 8.0 μV; $p = 0.028$). There was no correlation between oVEMP peak amplitudes and z-degree values of the cerebellum and posterior insula/parietal operculum (non-parametric Spearman-Rho correlation p always > 0.24); the same holds for cVEMPs (p always > 0.19). SVV did not show pathologic tilts (>2.5°) and did not differ between patients and controls, neither dynamic nor static SVV.

The Clinical Vestibular Score (CVS) revealed on average 10.2 ± 4.3. Subjective visual vertical in BVF patients was not different from controls (patients: 0.2° ± 2.6°; controls: 0.6° ± 1.2°; two-sample t-test $p = 0.61$). Subjective disease-related impairment for the Vertigo Handicap Questionnaire (VHQ) revealed on average 30.1 ± 19.1, for the Vertigo Symptom Scale (VSS) on average 35.0 ± 22.7 and the Subjective Dizziness Score (SDS) on average 13.1 ± 8.4. SDS was highly correlated ($r > 0.6$; $p < 0.01$) with the CVS, VHQ and VSS. There was no correlation of any of these scores to disease duration.

3.2. Altered intrinsic functional connectivity

Between-group differences in the voxel-degree obtained in the random effects analysis are summarized in Fig. 2 and Table 1. Patients showed lower functional connectivity of the posterior insula and parietal operculum bilaterally (CTR > BVF in Fig. 2A; Table 1A) and a higher connectivity in the cerebellum (BVF > CTR in Fig. 2B; Table 1B). The anatomical assignment was derived from the location of local cluster maxima, i.e., brain regions where we observed the strongest between-group effects.

We used cytoarchitectonic probability maps of the parietal operculum (SII) and the insular cortex from the SPM Anatomy toolbox (Eickhoff et al., 2005) to specify the anatomical location of our findings. 12% of the left cluster overlapped with the insular gyrus II (covering 39% of this region) and 8% with the parietal operculum areaOP4 (covering 7%). For the right cluster we found an overlap of 4% with the parietal operculum area OP4 (covering 4%) and of 3% with area OP3 (covering 6%). The remaining voxels (80% for the left hemisphere and 93% for the right hemisphere) comprising the cluster were located in the superior temporal gyrus and more anterior regions of the operculum.

Applying cytoarchitectonic probability maps of the cerebellum (Eickhoff et al., 2005), we found that 36% of the cluster in the left cerebellar hemisphere is assigned to the left lobule VIIa Crus II. 17% of the cluster in the right cerebellar hemisphere is located in the lobule VIIa Crus I and 16% in the lobule VI. The remaining voxels are distributed over other regions of the cerebellum. We only quote cerebellar regions where we found more than 10% of the voxels.

We repeated the analysis excluding the two patients with cerebellar ataxia and identified the same clusters (left hemisphere: adjusted p-value 0.036, cluster maximum −27 −72 −42 mm; right hemisphere: adjusted p-value 0.036, cluster maximum 30 −48 −39 mm). Therefore we conclude that our results are not driven by the BVF patients with cerebellar signs.

The mean degree in the clusters in which we found significant degree differences between BVF patients and healthy controls did not correlate with the disease duration (Pearson's linear correlation; all $p > 0.1$).

3.3. Investigation of underlying network changes

We performed seed-based functional connectivity analyses investigating four seed regions located in the posterior insula. Note that we followed a purely descriptive approach to gain a deeper understanding of the underlying network changes indicated by the differences in the voxel-degree. Fisher z-transformed functional connectivity maps for the control (CTR) and the patient (BVF) group are shown in Fig. 3A. The spherical seed region with a radius of 6 mm was placed in the right posterior insula (MNI coordinates of ROI center 42 −9 3 mm). Fig. 3A shows the between-group effects in functional connectivity according to a two-sample t-test. As a cut-off for the descriptive analysis of the between group effects a cluster defining threshold of $p = 0.001$

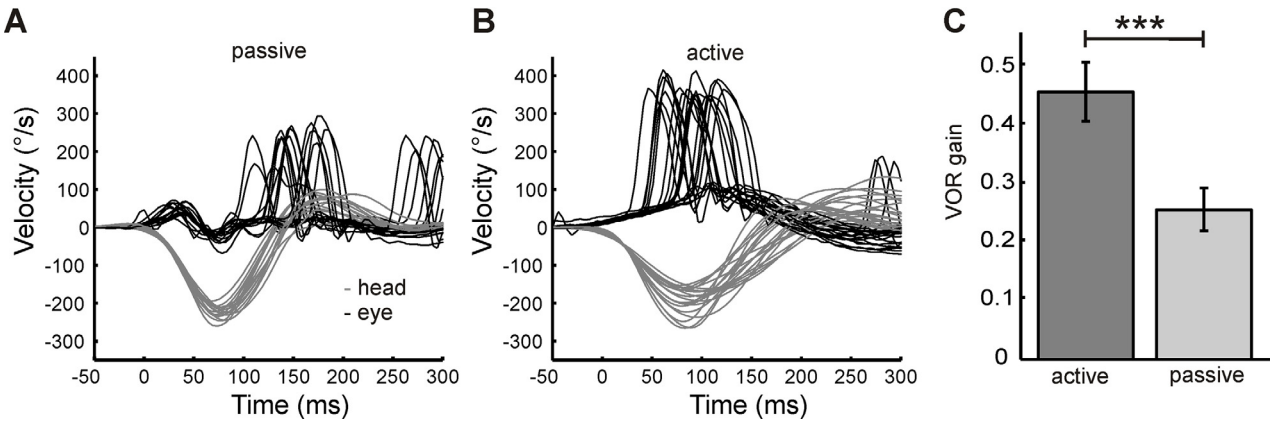

Fig. 1. Quantitative head thrust test. Eye and head velocity traces of the passive (A) and active (B) head impulse test of a single BVF patient are shown. (C) Vestibulo-ocular reflex (VOR) gain (mean ± standard error) of all BVF patients was significantly larger during active as compared to non-predictive passive head impulses (paired *t*-test; $p = 0.0001$).

Table 1
Between-group differences (BVF patients vs. healthy controls) in degree centrality.

Anatomical region		*p* (adj.) (cluster)	*k*	Local maxima [mm]			*T* (peak)
				x	*y*	*z*	
A) CTR > BVF							
Posterior insula	R	0.003	132	33	−3	−9	4.62
Parietal operculum	R			48	0	6	4.48
Posterior insula	R			42	−9	3	3.70
Posterior insula	L	0.002	161	−48	−9	6	4.36
Parietal operculum	L			−36	−15	6	4.17
Superior temporal gyrus	L			−54	−3	−12	4.02
B) BVF > CTR							
Cerebellum	R	0.043	79	−15	−72	−39	4.10
				−27	−72	−42	4.07
				−9	−69	−33	3.54
Cerebellum	L	0.019	108	27	−48	−39	4.00
				21	−66	−42	3.85
				30	−66	−39	3.58

Notes: Clusters with differences in the voxel degree between patients and controls (cluster defining threshold $p < 0.005$; topological FDR-correction). Anatomical region, adjusted cluster level probability and number of voxels per cluster (*k*) are listed. The table shows 3 local maxima (MNI coordinates) more than 8.0 mm apart and the peak *T*-scores.

and a cluster size of $k > 50$ were chosen. We tested for higher connectivity in the control group with respect to patients (CTR > BVF) as suggested by the higher degree of connectivity in the posterior insula found in the control group. Controls showed a stronger connectivity of the posterior insula (right) to the anterior insula (left), precuneus (right), cingulate cortex and the inferior/middle frontal gyrus (bilateral) (Table 2). We applied the same analysis approach to three other seed regions in the posterior insula (Fig. 3B). Each color represents the pattern of significantly altered connectivity for an individual seed region (cluster defining threshold $p = 0.001$; cluster size $k > 50$). The locations (MNI coordinates) of the four seed regions (Fig. 3B; on the right) had the following MNI coordinates: 1) ROI center 42 −9 3 mm (red); 2) ROI center −36 −15 6 mm (Rerkpattanapipat et al., 2009); 3) ROI center −48 −9 6 mm (green); and 4) ROI center 48 0 6 mm (yellow).

We repeated the seed-based connectivity analysis by decreasing the radius of the spherical seed regions to $r = 4$ mm and found that this did not affect our results.

3.4. Relationship to the VOR gain improvement

We performed a whole brain voxel-wise regression analysis to investigate if the degree centrality is modulated by the VOR gain difference (active minus passive). There was a striking positive correlation of this context-dependent VOR gain difference (active minus passive non-predictive VOR) to the degree centrality in the right supramarginal gyrus (Fig. 4A; Table 3), cerebellum, and straight gyrus (Fig. 4A; topological FDR correction; cluster defining threshold $p = 0.005$; 0.05 FDR-corrected cluster size was $k = 74$). These brain regions showed a stronger connectivity to the rest of the brain the larger the VOR gain was increased in the active HIT, i.e., connectivity increased as the difference between active and passive predictive VOR gain became larger. The cluster in the SMG contained 88 voxels. Thirty-eight percent of the voxels overlapped with the cytoarchitectonic region PFm of the supramarginal gyrus (Caspers et al., 2006) (covering 13% of this region) and 17% with the PFcm region (covering 16%). Applying cytoarchitectonic probability maps of the cerebellum (Diedrichsen et al., 2009; Eickhoff et al., 2005), we found that 49% of the cluster in the cerebellum is assigned to the lobule VIIa Crus I and 46% to the lobule VIIa Crus II.

For all subjects we extracted the mean z-degree in two clusters (SMG and cerebellum) where we observed a significant correlation between the functional connectivity (z-degree) and the VOR gain difference. Fig. 4B shows the interrelation between the mean z-degree and the VOR gain difference (active–passive) for BVF patients.

In an exploratory approach, we tested if the degree centrality is correlated to the VHQ or the VSS. There was no correlation between

Table 2
Functional connectivity of the right posterior insular cortex in healthy controls compared to BVF patients as depicted in Fig. 3A.

Anatomical region	*k*	*T* (peak)	Local maxima [mm]		
			x	*y*	*z*
Inferior/middle frontal gyrus (left)	228	4.34	−42	30	15
		4.13	−33	36	39
		4.06	−42	12	9
Inferior/middle frontal gyrus (right)	108	4.97	45	27	21
		3.62	30	33	33
Dorsal anterior cingulate cortex	96	4.63	6	3	30
		3.95	−3	6	27
		3.94	0	15	27
Precuneus (right)	56	4.38	9	−60	51
		4.07	3	−69	51

Notes: the table shows 3 local maxima (MNI coordinates) more than 8.0 mm apart, the cluster size*k* and the peak *T*-scores. Note that this is the results of a descriptive analysis investigating the higher connectivity observed in the posterior insula.

Table 3
Correlation between VOR gain difference (active–passive VOR) and the voxel-degree (differences BVF patients vs. controls).

Anatomical region	*p* (adj.) (cluster)	*k*	Local maxima [mm]			*T* (peak)
			x	*y*	*z*	
Cerebellum (right)	0.013	114	21	−84	−45	5.28
			21	−81	−30	4.88
			24	−75	−36	4.18
Supramarginal gyrus (right)	0.027	88	45	−45	33	4.70
			45	−33	30	4.33
			51	−42	27	4.29
Gyrus rectus	0.040	74	−3	42	−24	4.87
			15	33	−27	4.32
			18	24	−27	3.72

Notes: Clusters showing a positive correlation of the z-degree to the VOR gain difference (cluster defining threshold $p < 0.005$; topological FDR-correction; FDR-corrected critical cluster size was $k = 74$). Anatomical region, adjusted cluster level probability and number of voxels per cluster (k) are listed. The table shows 3 local maxima (MNI coordinates) more than 8.0 mm apart and the peak *T*-scores.

the degree centrality and these disease-related disability scores. Note, that the two scores are strongly correlated (Pearson's linear correlation coefficient $r = 0.6$; $p = 0.029$), i.e., not statistically independent.

4. Discussion

In contrast to previous brain imaging studies on vestibular disease, which largely used stimulus-related fMRI or PET designs, we used a data driven approach to investigate whole-brain resting-state functional connectivity in patients with chronic bilateral vestibular failure (BVF) compared to healthy controls. Most network analyses depend on a given parcellation of the brain, e.g., brain regions based on the SPM AAL template (Tzourio-Mazoyer et al., 2002). However, our voxel-based approach is not biased by an a priori hypothesis confined to defined anatomical structures and has a higher spatial resolution.

As a main result we found reduced functional connectivity of the posterior insula, parietal operculum and the superior temporal gyrus compared to healthy control subjects. These areas belong to vestibular cortex regions integrating multisensory signals into a percept of spatial orientation and self-motion. Importantly, these changes were found in BVF patients at rest, i.e., without any vestibular stimulation, which indicates a much more fundamental disease-related change in the resting brain: a change of resting-state connectivity. This reduced connectivity may be related to the poor prognosis of vestibular rehabilitation in BVF. Interestingly, however, one feasible clinical implication comes from the improvement of context-dependent, i.e., self-guided vestibular behavior with increasing connectivity in vestibular cortical areas (supramarginal gyrus, inferior parietal lobe) of BVF patients.

4.1. Functional connectivity of the posterior insula and the parietal operculum

We found reduced functional connectivity in the posterior insula, superior temporal gyrus and the parietal operculum. Pioneer animal work identified vestibular responses in the parieto-insular vestibular cortex (PIVC) in the posterior insula of the monkey (Grusser et al., 1990; Guldin and Grusser, 1998). Additional vestibular responses were found in animal experiments in adjacent retroinsular areas, the ventral intraparietal area in the fundus of the intraparietal sulcus (Bremmer et al., 2002). These regions showed increased neural activity (fMRI) during various vestibular (e.g., caloric, galvanic) stimuli in healthy human subjects. Specifically the middle and posterior insula, inferior parietal cortex, and posterior parietal cortex belong to multisensory cortical areas processing vestibular information (Becker-Bense et al., 2013; Bense et al., 2001; Dieterich et al., 2003; Emri et al., 2003; Fasold et al., 2002; Lobel et al., 1998; Lopez and Blanke, 2011; Naito et al., 2003; Seemungal et al., 2009; Stephan et al., 2005; Suzuki et al., 2001). Electrical stimulation in a lateral temporo-parietal area in humans elicited rotatory sensations (Kahane et al., 2003). STG and IPL also revealed structural changes in gray matter volume in unilateral vestibular failure patients (Helmchen et al., 2009; Helmchen et al., 2011).

In a PET study on BVF patients, task-independent metabolism

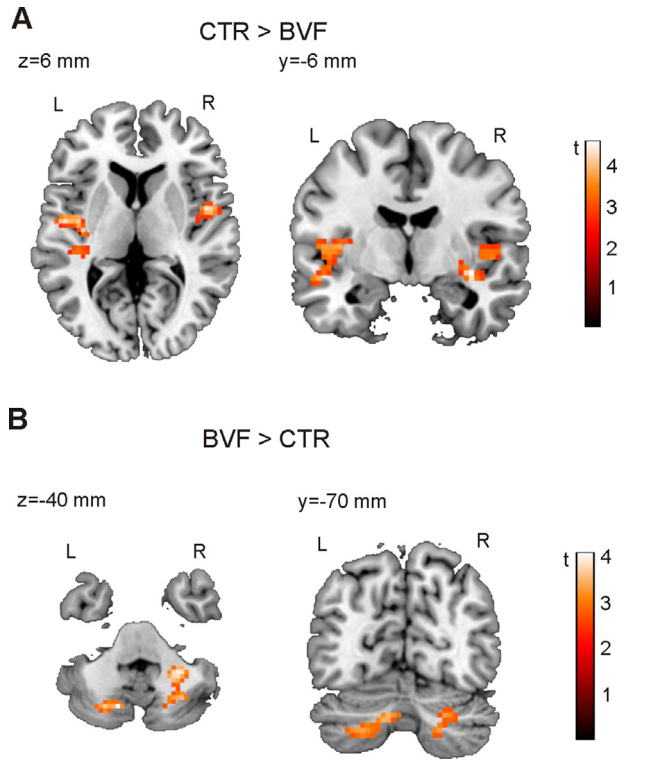

Fig. 2. Between-group effects in resting-state connectivity (expressed by the degree centrality). Statistical images were assessed for cluster-wise significance using a cluster defining threshold of $p = 0.005$ applying a topological $q = 0.05$ FDR-correction. Regions with increases in connectivity (as indicated by a larger degree centrality) in healthy controls (CTR) compared to patients (BVF) are shown in (A); regions with a larger connectivity in patients compared to controls in (B).

was strongly reduced in posterior insula (Bense et al., 2004b). Patients with bilateral vestibular hypofunction need to engage other sensory systems to compensate for deficient gaze stability, gait control, self-motion perception and spatial orientation. For this reason not only vestibular but also other sensory (visual, somatosensory) stimuli have been used to investigate the brain's responses to peripheral vestibular failure. Neural activity of cortical reciprocal inhibitory visual–vestibular interaction was changed: neural activity in the posterior insula and parietal operculum was decreased during caloric vestibular stimulation and concurrent deactivations in the visual cortex were absent or reduced in BVF (Bense et al., 2004b). In the same region (posterior insula) and the parietal operculum as well as superior temporal gyrus we found decreased bilateral functional connectivity compared to healthy controls. This reduction may affect reciprocal inhibitory visual–vestibular interaction which is normally required for spatial orientation and motion perception. On a behavioral level, distressing oscillopsia in BVF patients can be reduced by changing the cortical sensitivity of motion perception (Grunbauer et al., 1998; Kalla et al., 2011). Using a motion coherence paradigm, BVF patients showed raised thresholds of motion detection (Kalla et al., 2011). This has been taken as an adaptive process to compensate for oscillopsia. On the other hand, activations of the primary visual cortex and motion-sensitive areas V5 in the middle and inferior temporal gyri during optokinetic stimulation were significantly larger than those of age-matched healthy controls (Dieterich et al., 2007b). An upregulation of the visual sensitivity has been suggested and interpreted as a substitutional mechanism to compensate for deficient vestibular function. Our analysis did not show changes of connectivity in the visual cortex as a potential cause for altered responsiveness to visual motion.

The core vestibular region, OP2, primarily processes vestibular information but does not necessarily represent a multisensory area (Zu Eulenburg et al., 2012). In contrast, the posterior insula responds to multisensory stimulation (Zu Eulenburg et al., 2013). Thus, one reason for decreased cortical responses to vestibular stimulation in BVF patients (Bense et al., 2004b) may be reduced connectivity in OP2 and neighboring posterior insular areas at rest. It remains open at present whether this is a consequence of long lasting cortical deprivation from vestibular stimuli in BVF or whether this constitutes a secondary mechanism related to the poor vestibular rehabilitation in these patients.

4.2. Reduced connectivity of posterior insula: targets and physiological role

To gain a deeper understanding of the underlying network changes we investigated seed-based functional connectivity maps with seeds in the posterior insula. Any seed-based functional connectivity analyses in regions of degree differences are biased. It should be stressed that we followed a purely data-driven descriptive approach to investigate which brain regions are involved in the observed degree differences.

The seed-based analysis showed diminished connectivity from the posterior insula of BVF patients to the middle frontal gyrus, anterior cingulate cortex (ACC) and superior parietal lobule comprising the precuneus (Table 2). Apart from the posterior insula, the parietal operculum and the superior temporal gyrus, the precuneus and the ACC are repeatedly activated during vestibular stimulation (Dieterich and Brandt, 2008b; Zu Eulenburg et al., 2012). Our data complements and extends these findings by showing that the corresponding neural networks are affected which cannot be derived from the simple observation of co-activation alone.

The dorsal anterior insula has cortical projections to brain regions involved in executive functions and cognitive control (Deen et al., 2011), e.g., the anterior cingulate cortex (ACC) (Dosenbach et al., 2007) which might help to monitor errors and mismatches resulting from multisensory, i.e., somatosensory, interoceptive and vestibular information from the posterior insula (Corbetta et al., 1993). By detecting a mismatch between expected and actual vestibular feedback or by receiving contradicting information from different sensory systems, the ACC may facilitate decision making processes to adapt behavior and may mediate context-driven modulation of bodily arousal states (Critchley et al., 2003). Although there is some human and animal data supporting a role of ACC, specifically Brodmann area 24 in the interface of motor control, arousal/drive state and cognition (Paus, 2001), which makes ACC a potential candidate to translate intentions to actions, data are required to show that this interface operates sufficiently fast to modulate a vestibular driven motor behavior with such a short latency as the vestibulo-ocular reflex.

The precuneus (Brodmann area 7) was shown to be activated during caloric vestibular stimulation (Dieterich et al., 2003; Dieterich and Brandt, 2008b). According to monkey data, area 7 showed structural connections with subcortical regions involved in vestibulo-ocular function (Faugier-Grimaud and Ventre, 1989; Ventre and Faugier-Grimaud, 1986). Thus there is some evidence for a role of the precuneus in the cortical vestibular circuit.

We conclude that our data suggests that enduring deficient or missing vestibular input weakens the functional connectivity within the vestibular cortical network.

As the threshold of our descriptive analysis is arbitrary, we repeated the seed based analysis by changing the p-threshold to $p = 0.005$ and looked for consistent effects. For all four seed regions we found the hippocampus (left and right hemispheres) to be consistently more connected to the posterior insula in the control group compared to patients. This extends previous observations by Brandt and co-workers of structural changes of the hippocampus

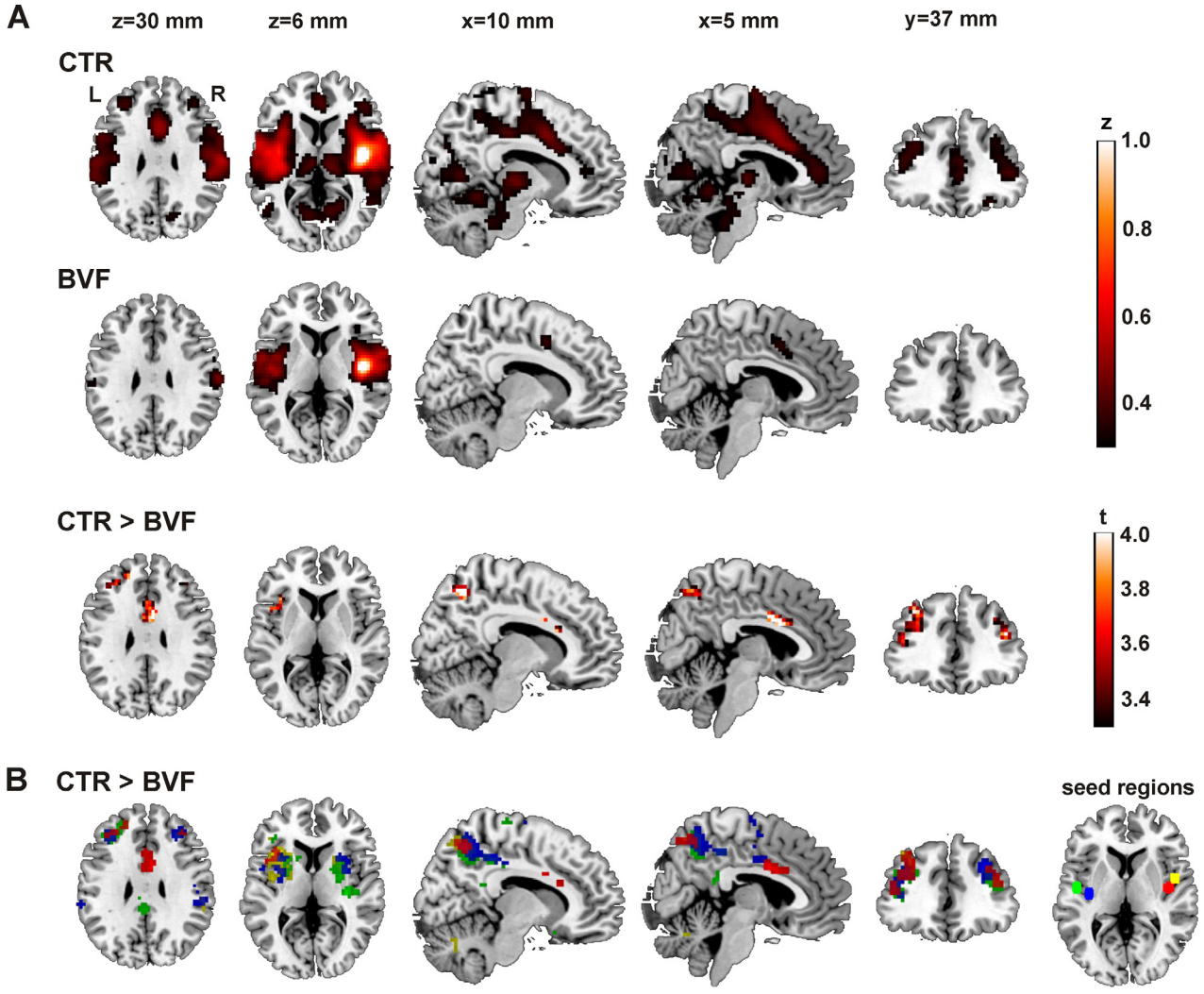

Fig. 3. Seed-based functional connectivity analyses with seed regions located in the posterior insula. A) Fisher z-transformed functional connectivity maps for the control (CTR; first row) and patient (BVF; second row) groups. The spherical seed region with a radius of 6 mm was located in the right posterior insula (MNI coordinates of ROI center 42 −9 3 mm). Between-group effects in functional connectivity (CTR > BVF) are shown in the third row. B) Between-group effects for four different seed regions in the posterior insula are shown for the contrast CTR > BVF (red: ROI center 42 −9 3 mm; blue: ROI center −36 −15 6 mm; green: ROI center −48 −9 6 mm; yellow: ROI center 48 0 6 mm).

of BVF patients who also exhibited spatial memory and navigation deficits (Brandt et al., 2005). Our data provide additional pieces of evidence for a neural correlate of impaired spatial orientation in BVF. Furthermore, we selected different seed-regions in the parietal operculum and posterior insula and showed that the connectivity patterns for the different seed regions converge.

4.3. Increased cerebellar functional connectivity in BVF

Interestingly, our BVF patients showed a higher connectivity in the cerebellum compared to healthy controls. The cerebellar region Crus I showed functional resting state connectivity with the dorsolateral prefrontal cortex, the inferior parietal lobule, pre-supplementary motor area and the anterior cingulate cortex (Buckner et al., 2011). The cerebellar region at the border of Crus I/II is functionally connected with cerebral regions related to the default mode network (posterior cingulate cortex, lateral temporal cortex, inferior parietal lobule and medial prefrontal cortex) (Buckner et al., 2011). Bernard et al. (2012) found that the cerebellar region Crus I is functionally connected to the superior frontal gyrus (frontal eye fields) and the angular gyrus in the inferior parietal cortex which represents awareness that an intended action is consistent with movement consequences and the awareness of the authorship of the action (Farrer et al., 2008). It is intriguing to speculate that this increased cerebellar connectivity indicates compensatory substitutional processes to improve the awareness of self-initiated movements or contributes to an improved coordination between parietal and frontal eye fields. Some support comes from the fact that functional connectivity in this cerebellar region correlates with the degree by which self-guided (active) VOR gets larger when compared with passive VOR (see below).

4.4. Relation of changes in functional connectivity and clinical performance

Seventy percent of BVF patients do not show spontaneous improvement over time (Zingler et al., 2008). Unlike UVF patients (Helmchen et al., 2013), who usually recover, it is less promising to relate clinical consecutive recordings in BVF to follow-up imaging data. Therefore we related changes of functional connectivity to a context-dependent vestibular behavior in BVF. By comparing the VOR gain during active and passive head movements we found that BVF patients can impressively increase their VOR gain if head-movements are actively performed. Interestingly, functional connectivity in the supramarginal gyrus, the rostro-dorsal part of the inferior parietal

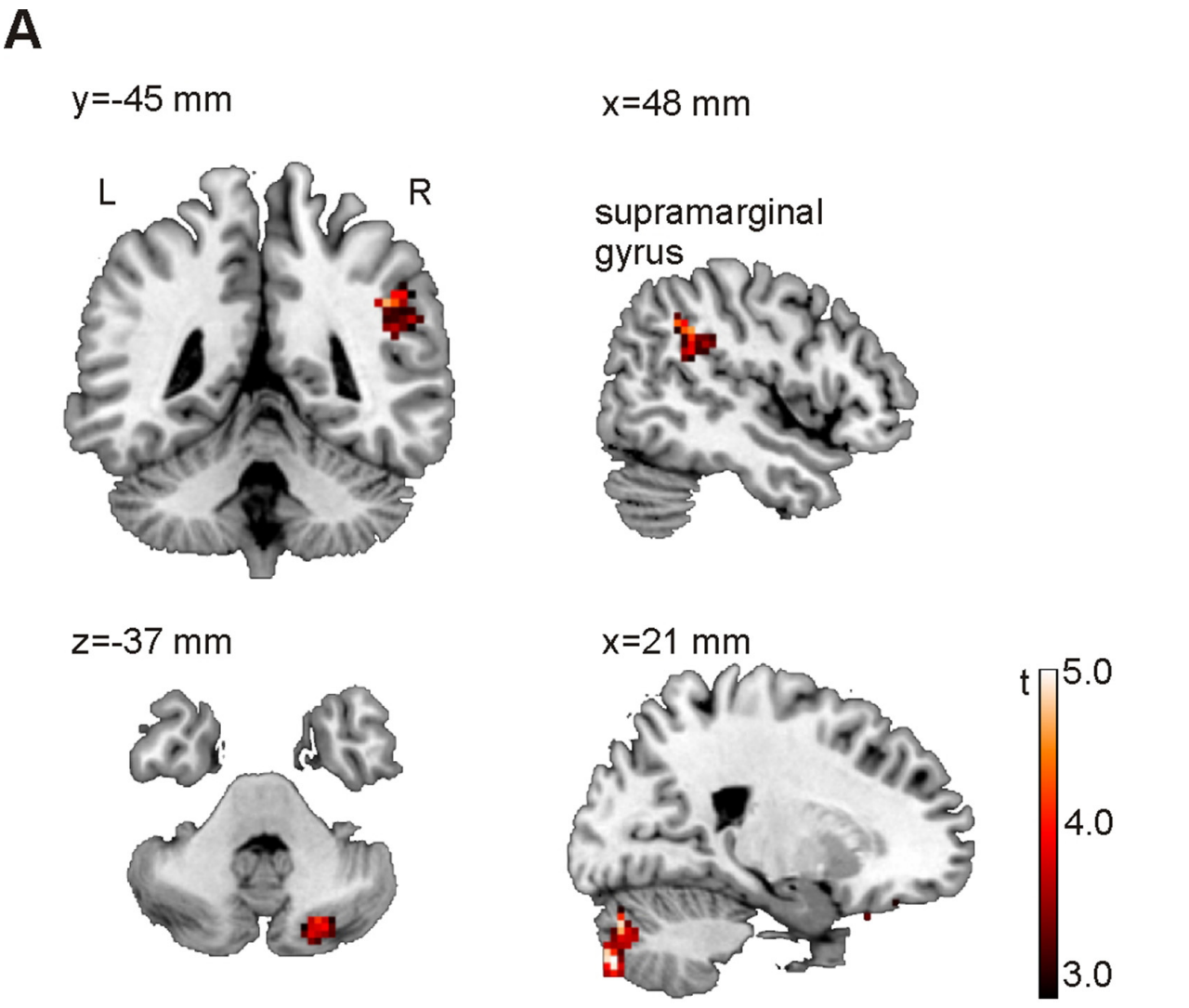

Fig. 4. Interrelation between the connectivity (z-degree) and the VOR gain difference. A) Brain regions with a positive correlation between connectivity (z-degree) and context-dependent (active–passive) VOR gain differences are shown (cluster defining threshold $p < 0.005$; topological FDR-correction; FDR-corrected critical cluster size was $k = 74$). B) Interrelation between the mean connectivity (z-degree) and the VOR gain difference (active–passive VOR gain) for BVF patients. The larger the differences between active vs. passive VOR gain the larger the regional increase in connectivity in the supramarginal gyrus (upper panel) and cerebellum (lower panel). The mean z-degree was extracted from the clusters in which there was a significant correlation between the z-degree and the VOR gain difference.

lobe, correlated with the context-dependent increase in the vestibulo-ocular performance, i.e., the larger the increase of VOR gain difference between active and passive head movements the larger was the increase in functional connectivity in this region. In contrast, changes of functional connectivity in these regions were not related to otolith dysfunction.

The supramarginal gyrus (SMG) belongs to the inferior parietal lobule which is a cortical multisensory integration area (Zu Eulenburg et al., 2012). In association with the superior temporal gyrus and the posterior insula it receives and integrates visual, vestibular and somatosensory information to construct a coherent spatial orientation (Angelaki and Cullen, 2008; Lopez and Blanke, 2011). This has been corroborated by human cortical lesion studies (Baier et al., 2012), electrical stimulation studies (Kahane et al., 2003) and functional imaging studies (Lopez et al., 2012). Its implication for vestibular processing has been shown not only in event-related stimulation studies but also at rest. We recently found decreased functional connectivity in SMG and adjacent intraparietal sulcus in acute unilateral vestibular neuritis patients which recovered over time as individual vestibular-induced disability improved (Helmchen et al., 2013). Additional evidence for multisensory integration of the SMG comes from a recent transcranial magnetic stimulation (TMS) study. TMS of the supramarginal gyrus in healthy human subjects selectively elicited tilts of the subjective visual vertical (SVV), a perceptional correlate of our static upright reference (Kheradmand et al., 2013a). It is generated by the integration of vestibular, visual and proprioceptive signals which can be pathologically tilted by cortical lesions (Brandt and Dieterich, 1994). This supports a role of SMG in multisensory integration to establish an accurate upright perception. The lateralization, i.e., the right-sided increase in functional connectivity in our BVF patients with active vs. passive head movements is compatible with the specialization of the right human hemisphere in spatial orientation and its dominance in vestibular processing (Dieterich et al., 2003; Fink et al., 2003). A common reference system for spatial orientation can only be derived from a transformation of the different coordinate frames of the different sensory systems. The SMG but not the posterior insula has been shown to contribute to this internal reference of upright perception (SVV) and spatial orientation (Kheradmand et al., 2013b). Moreover, not only the SVV but also the VOR may become asymmetric by right-sided cortical temporoparietal lesions in patients involving the SMG (Ventre-Dominey et al., 2003).

The adjacent ventral intraparietal area (VIP) contains neural representations of self-motion based on vestibular and visual signal integration (Chen et al., 2011). It contains neurons that respond to head-movement related signals in relation to passive and active movements (Klam and Graf, 2003b). The variety of neuronal responses ranging from total extinction to activity only during active head movements suggests a role of VIP in sensory space representation (Klam and Graf, 2003a). The posterior parietal cortex and the vestibular nuclei are likely candidates to contribute to the distinction between active and passive head movements since the peripheral vestibular receptors cannot (Roy and Cullen, 2004). Sensory space representation is influenced by non- or extra-vestibular inputs such as motor efference copy signals of the neck and head motor command and the proprioceptive feedback signal. They allow to predict the gaze error and may substitute for the bilateral loss of vestibular information to stabilize gaze during head movements by, e.g. preprogramming compensatory eye movements (Della Santina et al., 2002) or by increasing the weight of neck motor efference copy which can be sufficient to explain improvements in gaze stability during active self-motion (Sadeghi et al., 2012). The increased intrinsic connectivity with increasing VOR gain during active head movements in BVF implies a functional role of the SMG in the sensory substitution and integration of motor efference copy signals.

Interestingly, the posterior cerebellum similarly showed increasing functional connectivity with increasing VOR gain during active head movements. Vestibular nucleus neurons encoding the difference between the expected reafference and the sensory consequence of the actual movement project to the cerebellum which is probably involved in anticipating VOR responses (King, 2013). The cerebellar role in anticipating sensory consequences of motor behavior is well established (Ploghaus et al., 1999) and one might speculate that increased cerebellar functional connectivity in our BVF patients helped to predict their own gaze error and to elicit a compensatory, stronger eye velocity signal with active HIT. Intrinsic functional connectivity studies have recently demonstrated strong functional cerebello-cerebral connectivity of the visual and sensorimotor network, specifically from cerebellar lobule VI to the inferior parietal lobe (Kipping et al., 2013) and from cerebellar Crus I to the superior frontal gyrus (frontal eye fields) and the angular and supramarginal gyrus (Bernard et al., 2012). A stronger connectivity to the frontal eye fields and the SMG may facilitate better performance of gaze stabilization in the passive HIT condition. Future connectivity studies will have to investigate whether this cerebello-cerebral functional connectivity to the inferior parietal lobe can be modulated to improve vestibular rehabilitation in BVF.

5. Conclusions

Our study provides first evidence that there is a strong change in resting-state activity even without vestibular stimulation indicating profound behavioral task-independent changes in resting-state functional connectivity of BVF patients. Our data driven approach revealed decreased functional connectivity of the posterior insula (PI) and the parietal operculum (OP) in BVF patients. These regions are multisensory regions processing somatosensory, nociceptive and vestibular information which have been identified as core regions of vestibular cortical processing in hypothesis-driven event-related activation studies. These regions can now be used as seed regions to identify the directions and targets of these altered connectivity and their relation to levels of functional impairments in vestibular disease.

Acknowledgments

This work was supported through intramural funding of the University of Lübeck. UMK and TFM receive support from the DFG.

References

Alessandrini, M., Napolitano, B., Bruno, E., Belcastro, L., Ottaviani, F., Schillaci, O., 2009. Cerebral plasticity in acute vestibular deficit. European Archives of Oto-rhino-laryngology: Official Journal of the European Federation of Oto-Rhino-Laryngological Societies (EUFOS): Affiliated With the German Society for Oto-Rhino-Laryngology - Head and Neck Surgery 266, 1547–1551. http://dx.doi.org/10.1007/s00405-009-0953-4, 19294399.

Angelaki, D.E., Cullen, K.E., 2008. Vestibular system: the many facets of a multimodal sense. Annual Review of Neuroscience 31, 125–150. http://dx.doi.org/10.1146/annurev.neuro.31.060407.125555, 18338968.

Baier, B., Thomke, F., Wilting, J., Heinze, C., Geber, C., Dieterich, M., 2012. A pathway in the brainstem for roll-tilt of the subjective visual vertical: evidence from a lesion-behavior mapping study. Journal of Neuroscience 32, 14854–14858. http://dx.doi.org/10.1523/JNEUROSCI.0770-12.2012.

Becker-Bense, S., Dieterich, M., Buchholz, H.G., Bartenstein, P., Schreckenberger, M., Brandt, T., 2013. The differential effects of acute right- vs. left-sided vestibular failure on brain metabolism. Brain Structure & Function, 5–6, 23686397.

Bense, S., Bartenstein, P., Lochmann, M., Schlindwein, P., Brandt, T., Dieterich, M., 2004. Metabolic changes in vestibular and visual cortices in acute vestibular neuritis. Annals of Neurology 56, 624–630. http://dx.doi.org/10.1002/ana.20244, 15449325.

Bense, S., Deutschländer, A., Stephan, T., Bartenstein, P., Schwaiger, M., Brandt, T. et al, 2004. Preserved visual–vestibular interaction in patients with bilateral vestibular failure. Neurology 63, 122–128. http://dx.doi.org/10.1212/01.WNL.0000129545.79566.6A, 15249621.

Bense, S., Stephan, T., Yousry, T.A., Brandt, T., Dieterich, M., 2001. Multisensory cortical signal increases and decreases during vestibular galvanic stimulation (fMRI). Journal of Neurophysiology 85, 886–899, 11160520.

Bernard, J.A., Seidler, R.D., Hassevoort, K.M., Benson, B.L., Welsh, R.C., Wiggins, J.L. et al, 2012. Resting state corticocerebellar functional connectivity networks: a comparison of anatomical and self-organizing map approaches. Frontiers in Neuroanatomy 6, 31–, 22907994.
Beucke, J.C., Sepulcre, J., Talukdar, T., Linnman, C., Zschenderlein, K., Endrass, T. et al, 2013. Abnormally high degree connectivity of the orbitofrontal cortex in obsessive-compulsive disorder. JAMA Psychiatry 70, 619–629. http://dx.doi.org/10.1001/jamapsychiatry.2013.173, 23740050.
Biswal, B., Yetkin, F.Z., Haughton, V.M., Hyde, J.S., 1995. Functional connectivity in the motor cortex of resting human brain using echo-planar MRI. Magnetic Resonance in Medicine: Official Journal of the Society of Magnetic Resonance in Medicine / Society of Magnetic Resonance in Medicine 34, 537–541. http://dx.doi.org/10.1002/mrm.1910340409, 8524021.
Black, R.A., Halmagyi, G.M., Thurtell, M.J., Todd, M.J., Curthoys, I.S., 2005. The active head-impulse test in unilateral peripheral vestibulopathy. Archives of Neurology 62, 290–293. http://dx.doi.org/10.1001/archneur.62.2.290, 15710858.
Brandt, T., 1996. Bilateral vestibulopathy revisited. European Journal of Medical Research 1, 361–368, 9360934.
Brandt, T., Dieterich, M., 1994. Vestibular syndromes in the roll plane: topographic diagnosis from brainstem to cortex. Annals of Neurology 36, 337–347. http://dx.doi.org/10.1002/ana.410360304, 8080241.
Brandt, T., Schautzer, F., Hamilton, D.A., Brüning, R., Markowitsch, H.J., Kalla, R. et al, 2005. Vestibular loss causes hippocampal atrophy and impaired spatial memory in humans. Brain: a Journal of Neurology 128, 2732–2741. http://dx.doi.org/10.1093/brain/awh617, 16141283.
Bremmer, F., Klam, F., Duhamel, J.R., Ben, Hamed S., Graf, W., 2002. Visual–vestibular interactive responses in the macaque ventral intraparietal area (VIP). European Journal of Neuroscience 16, 1569–1586. http://dx.doi.org/10.1046/j.1460-9568.2002.02206.x, 12405971.
Buckner, R.L., Krienen, F.M., Castellanos, A., Diaz, J.C., Yeo, B.T., 2011. The organization of the human cerebellum estimated by intrinsic functional connectivity. Journal of Neurophysiology 106, 2322–2345. http://dx.doi.org/10.1152/jn.00339.2011, 21795627.
Buckner, R.L., Sepulcre, J., Talukdar, T., Krienen, F.M., Liu, H., Hedden, T. et al, 2009. Cortical hubs revealed by intrinsic functional connectivity: mapping, assessment of stability, and relation to Alzheimer's disease. Journal of Neuroscience: the Official Journal of the Society for Neuroscience 29, 1860–1873. http://dx.doi.org/10.1523/JNEUROSCI.5062-08.2009, 19211893.
Bullmore, E., Sporns, O., 2009. Complex brain networks: graph theoretical analysis of structural and functional systems. Nature Reviews. Neuroscience 10, 186–198. http://dx.doi.org/10.1038/nrn2575, 19190637.
Caspers, S., Geyer, S., Schleicher, A., Mohlberg, H., Amunts, K., Zilles, K., 2006. The human inferior parietal cortex: cytoarchitectonic parcellation and interindividual variability. Neuroimage 33, 430–448. http://dx.doi.org/10.1016/j.neuroimage.2006.06.054, 16949304.
Chen, A., DeAngelis, G.C., Angelaki, D.E., 2011. Representation of vestibular and visual cues to self-motion in ventral intraparietal cortex. Journal of Neuroscience: the Official Journal of the Society for Neuroscience 31, 12036–12052. http://dx.doi.org/10.1523/JNEUROSCI.0395-11.2011, 21849564.
Chumbley, J., Worsley, K., Flandin, G., Friston, K., 2010. Topological FDR for neuroimaging. NeuroImage 49, 3057–3064. http://dx.doi.org/10.1016/j.neuroimage.2009.10.090, 19944173.
Chumbley, J.R., Friston, K.J., 2009. False discovery rate revisited: FDR and topological inference using Gaussian random fields. Neuroimage 44, 62–70. http://dx.doi.org/10.1016/j.neuroimage.2008.05.021, 18603449.
Corbetta, M., Miezin, F.M., Shulman, G.L., Petersen, S.E., 1993. A PET study of visuospatial attention. The Journal of Neuroscience: The Official Journal of the Society for Neuroscience 13, 1202–1226.
Critchley, H.D., Mathias, C.J., Josephs, O., O'Doherty, J., Zanini, S., Dewar, B.K. et al, 2003. Human cingulate cortex and autonomic control: converging neuroimaging and clinical evidence. Brain: a Journal of Neurology 126, 2139–2152. http://dx.doi.org/10.1093/brain/awg216, 12821513.
Curthoys, I.S., Vulovic, V., Manzari, L., 2012. Ocular vestibular-evoked myogenic potential (oVEMP) to test utricular function: neural and oculomotor evidence. Acta Otorhinolaryngologica Italica: Organo Ufficiale Della Società italiana Di Otorinolaringologia E Chirurgia Cervico-facciale 32, 41–45, 22500066.
Cutfield, N.J., Scott, G.P., Waldman, A.D., Sharp, D.J., Bronstein, A.M., 2014. Visual and proprioceptive interaction in patients with bilateral vestibular loss. NeuroImage: Clinical 4, 274–282. http://dx.doi.org/10.1016/j.nicl.2013.12.013.
Deen, B., Pitskel, N.B., Pelphrey, K.A., 2011. Three systems of insular functional connectivity identified with cluster analysis. Cerebral Cortex (New York, N.Y.: 1991) 21, 1498–1506. http://dx.doi.org/10.1093/cercor/bhq186, 21097516.
Della, Santina C.C., Cremer, P.D., Carey, J.P., Minor, L.B., 2002. Comparison of head thrust test with head autorotation test reveals that the vestibulo-ocular reflex is enhanced during voluntary head movements. Archives of Otolaryngology—head & Neck Surgery 128, 1044–1054. http://dx.doi.org/10.1001/archotol.128.9.1044, 12220209.
Diedrichsen, J., Balsters, J.H., Flavell, J., Cussans, E., Ramnani, N., 2009. A probabilistic MR atlas of the human cerebellum. NeuroImage 46, 39–46. http://dx.doi.org/10.1016/j.neuroimage.2009.01.045, 19457380.
Dieterich, M., Bauermann, T., Best, C., Stoeter, P., Schlindwein, P., 2007. Evidence for cortical visual substitution of chronic bilateral vestibular failure (an fMRI study). Brain: a Journal of Neurology 130, 2108–2116. http://dx.doi.org/10.1093/brain/awm130, 17575279.
Dieterich, M., Bauermann, T., Best, C., Stoeter, P., Schlindwein, P., 2007. Evidence for cortical visual substitution of chronic bilateral vestibular failure (an fMRI study). Brain: a Journal of Neurology 130, 2108–2116. http://dx.doi.org/10.1093/brain/awm130, 17575279.
Dieterich, M., Bense, S., Lutz, S., Drzezga, A., Stephan, T., Bartenstein, P. et al, 2003. Dominance for vestibular cortical function in the non-dominant hemisphere. Cerebral Cortex (New York, N.Y.: 1991) 13, 994–1007. http://dx.doi.org/10.1093/cercor/13.9.994, 12902399.
Dieterich, M., Brandt, T., 1993. Ocular torsion and tilt of subjective visual vertical are sensitive brainstem signs. Annals of Neurology 33, 292–299, 8498813.
Dieterich, M., Brandt, T., 2008. Functional brain imaging of peripheral and central vestibular disorders. Brain: a Journal of Neurology 131, 2538–2552. http://dx.doi.org/10.1093/brain/awn042, 18515323.
Dieterich, M., Brandt, T., 2008. Functional brain imaging of peripheral and central vestibular disorders. Brain: a Journal of Neurology 131, 2538–2552. http://dx.doi.org/10.1093/brain/awn042, 18515323.
Dosenbach, N.U., Fair, D.A., Miezin, F.M., Cohen, A.L., Wenger, K.K., Dosenbach, R.A. et al, 2007. Distinct brain networks for adaptive and stable task control in humans. Proceedings of the National Academy of Sciences of the United States of America 104, 11073–11078. http://dx.doi.org/10.1073/pnas.0704320104, 17576922.
Eickhoff, S.B., Stephan, K.E., Mohlberg, H., Grefkes, C., Fink, G.R., Amunts, K. et al, 2005. A new SPM toolbox for combining probabilistic cytoarchitectonic maps and functional imaging data. NeuroImage 25, 1325–1335. http://dx.doi.org/10.1016/j.neuroimage.2004.12.034, 15850749.
Emri, M., Kisely, M., Lengyel, Z., Balkay, L., Márián, T., Mikó, L. et al, 2003. Cortical projection of peripheral vestibular signaling. Journal of Neurophysiology 89, 2639–2646. http://dx.doi.org/10.1152/jn.00599.2002, 12740408.
Farrer, C., Frey, S.H., Van Horn, J.D., Tunik, E., Turk, D., Inati, S. et al, 2008. The angular gyrus computes action awareness representations. Cerebral Cortex (New York, N.Y.: 1991) 18, 254–261. http://dx.doi.org/10.1093/cercor/bhm050, 17490989.
Fasold, O., von Brevern, M., Kuhberg, M., Ploner, C.J., Villringer, A., Lempert, T. et al, 2002. Human vestibular cortex as identified with caloric stimulation in functional magnetic resonance imaging. Neuroimage 17, 1384–1393. http://dx.doi.org/10.1006/nimg.2002.1241, 12414278.
Faugier-Grimaud, S., Ventre, J., 1989. Anatomic connections of inferior parietal cortex (area 7) with subcortical structures related to vestibulo-ocular function in a monkey (*Macaca fascicularis*). Journal of Comparative Neurology 280, 1–14. http://dx.doi.org/10.1002/cne.902800102, 2465325.
Fink, G.R., Marshall, J.C., Weiss, P.H., Stephan, T., Grefkes, C., Shah, N.J. et al, 2003. Performing allocentric visuospatial judgments with induced distortion of the egocentric reference frame: an fMRI study with clinical implications. NeuroImage 20, 1505–1517. http://dx.doi.org/10.1016/j.neuroimage.2003.07.006, 14642463.
Göttlich, M., Münte, T.F., Heldmann, M., Kasten, M., Hagenah, J., Krämer, U.M., 2013. Altered resting state brain networks in Parkinson's disease. PLOS One 8.
Grünbauer, W.M., Dieterich, M., Brandt, T., 1998. Bilateral vestibular failure impairs visual motion perception even with the head still. Neuroreport 9, 1807–1810. http://dx.doi.org/10.1097/00001756-199806010-00025, 9665605.
Grüsser, O.J., Pause, M., Schreiter, U., 1990. Localization and responses of neurones in the parieto-insular vestibular cortex of awake monkeys (*Macaca fascicularis*). Journal of Physiology 430, 537–557, 2086773.
Guldin, W.O., Grüsser, O.J., 1998. Is there a vestibular cortex? Trends in Neurosciences 21, 254–259. http://dx.doi.org/10.1016/S0166-2236(97)01211-3, 9641538.
Helmchen, C., Klinkenstein, J., Machner, B., Rambold, H., Mohr, C., Sander, T., 2009. Structural changes in the human brain following vestibular neuritis indicate central vestibular compensation. Annals of the New York Academy of Sciences 1164, 104–115. http://dx.doi.org/10.1111/j.1749-6632.2008.03745.x, 19645887.
Helmchen, C., Klinkenstein, J.C., Krüger, A., Gliemroth, J., Mohr, C., Sander, T., 2011. Structural brain changes following peripheral vestibulocochlear lesion may indicate multisensory compensation. Journal of Neurology, Neurosurgery, and Psychiatry 82, 309–316. http://dx.doi.org/10.1136/jnnp.2010.204925, 20802221.
Helmchen, C., Ye, Z., Sprenger, A., Münte, T.F., 2013. Changes in resting-state fMRI in vestibular neuritis. Brain Structure & Function 2, 23881293.
Kheradmand, A., Lasker, A., Zee, D.S., 2013. Transcranial magnetic stimulation (TMS) of the supramarginal gyrus: a window to perception of upright. Cerebral Cortex (New York, N.Y.: 1991) 4, 24084127.
Jorns-Häderli, M., Straumann, D., Palla, A., 2007. Accuracy of the bedside head impulse test in detecting vestibular hypofunction. Journal of Neurology, Neurosurgery, and Psychiatry 78, 1113–1118. http://dx.doi.org/10.1136/jnnp.2006.109512, 17220287.
Kahane, P., Hoffmann, D., Minotti, L., Berthoz, A., 2003. Reappraisal of the human vestibular cortex by cortical electrical stimulation study. Annals of Neurology 54, 615–624. http://dx.doi.org/10.1002/ana.10726, 14595651.
Kalla, R., Muggleton, N., Spiegel, R., Bueti, D., Claassen, J., Walsh, V. et al, 2011. Adaptive motion processing in bilateral vestibular failure. Journal of Neurology, Neurosurgery, and Psychiatry 82, 1212–1216. http://dx.doi.org/10.1136/jnnp.2010.235960, 21551468.
Kheradmand, A., Lasker, A., Zee, D.S., 2013. Transcranial magnetic stimulation (TMS) of the supramarginal gyrus: a window to perception of upright. Cerebral Cortex (New York, N.Y.: 1991) 4, 24084127.
King, W.M., 2013. Getting ahead of oneself: anticipation and the vestibulo-ocular reflex. Neuroscience 236, 210–219. http://dx.doi.org/10.1016/j.neuroscience.2012.12.032, 23370320.
Kipping, J.A., Grodd, W., Kumar, V., Taubert, M., Villringer, A., Margulies, D.S., 2013. Overlapping and parallel cerebello-cerebral networks contributing to sensorimotor control: an intrinsic functional connectivity study. Neuroimage 83, 837–848. http://dx.doi.org/10.1016/j.neuroimage.2013.07.027, 23872155.
Klam, F., Graf, W., 2003. Vestibular response kinematics in posterior parietal cortex

neurons of macaque monkeys. European Journal of Neuroscience 18, 995–1010. http://dx.doi.org/10.1046/j.1460-9568.2003.02813.x, 12925025.
Klam, F., Graf, W., 2003. Vestibular signals of posterior parietal cortex neurons during active and passive head movements in macaque monkeys. Annals of the New York Academy of Sciences 1004, 271–282. http://dx.doi.org/10.1196/annals.1303.024, 14662466.
Lobel, E., Kleine, J.F., Bihan, D.L., Leroy-Willig, A., Berthoz, A., 1998. Functional MRI of galvanic vestibular stimulation. Journal of Neurophysiology 80, 2699–2709, 9819274.
Lopez, C., Blanke, O., 2011. The thalamocortical vestibular system in animals and humans. Brain Research Reviews 67, 119–146. http://dx.doi.org/10.1016/j.brainresrev.2010.12.002.
Lopez, C., Blanke, O., Mast, F.W., 2012. The human vestibular cortex revealed by coordinate-based activation likelihood estimation meta-analysis. Neuroscience 212, 159–179. http://dx.doi.org/10.1016/j.neuroscience.2012.03.028, 22516007.
Machner, B., Sprenger, A., Füllgraf, H., Trillenberg, P., Helmchen, C., 2013. [Video-based head impulse test. Importance for routine diagnostics of patients with vertigo]. Der Nervenarzt 84, 975–983. http://dx.doi.org/10.1007/s00115-013-3824-6, 23839059.
Naito, Y., Tateya, I., Hirano, S., Inoue, M., Funabiki, K., Toyoda, H. et al, 2003. Cortical correlates of vestibulo-ocular reflex modulation: a PET study. Brain: a Journal of Neurology 126, 1562–1578. http://dx.doi.org/10.1093/brain/awg165, 12805122.
Palla, A., Straumann, D., 2004. Recovery of the high-acceleration vestibulo-ocular reflex after vestibular neuritis. Journal of the Association for Research in Otolaryngology: JARO 5, 427–435. http://dx.doi.org/10.1007/s10162-004-4035-4, 15675005.
Paus, T., 2001. Primate anterior cingulate cortex: where motor control, drive and cognition interface. Nature Reviews. Neuroscience 2, 417–424. http://dx.doi.org/10.1038/35077500, 11389475.
Ploghaus, A., Tracey, I., Gati, J.S., Clare, S., Menon, R.S., Matthews, P.M. et al, 1999. Dissociating pain from its anticipation in the human brain. Science (New York, N.Y.) 284, 1979–1981. http://dx.doi.org/10.1126/science.284.5422.1979, 10373114.
Rerkpattanapipat, P., D'Agostino, R.B. Jr., Link, K.M., Shahar, E., Lima, J.A., Bluemke, D.A. et al, 2009. Location of arterial stiffening differs in those with impaired fasting glucose versus diabetes: implications for left ventricular hypertrophy from the Multi-Ethnic Study of Atherosclerosis. Diabetes 58, 946–953. http://dx.doi.org/10.2337/db08-1192, 19136657.
Rosengren, S.M., Kingma, H., 2013. New perspectives on vestibular evoked myogenic potentials. Current Opinion in Neurology 26, 74–80. http://dx.doi.org/10.1097/WCO.0b013e32835c5ef3, 23254558.
Rosengren, S.M., Welgampola, M.S., Colebatch, J.G., 2010. Vestibular evoked myogenic potentials: past, present and future. Clinical Neurophysiology: Official Journal of the International Federation of Clinical Neurophysiology 121, 636–651. http://dx.doi.org/10.1016/j.clinph.2009.10.016, 20080441.
Roy, J.E., Cullen, K.E., 2004. Dissociating self-generated from passively applied head motion: neural mechanisms in the vestibular nuclei. Journal of Neuroscience: the Official Journal of the Society for Neuroscience 24, 2102–2111. http://dx.doi.org/10.1523/JNEUROSCI.3988-03.2004, 14999061.
Sadeghi, S.G., Minor, L.B., Cullen, K.E., 2012. Neural correlates of sensory substitution in vestibular pathways following complete vestibular loss. Journal of Neuroscience: the Official Journal of the Society for Neuroscience 32, 14685–14695. http://dx.doi.org/10.1523/JNEUROSCI.2493-12.2012, 23077054.
Schmid-Priscoveanu, A., Böhmer, A., Obzina, H., Straumann, D., 2001. Caloric and search-coil head-impulse testing in patients after vestibular neuritis. Journal of the Association for Research in Otolaryngology: JARO 2, 72–78, 11545152.
Seemungal, B.M., Rizzo, V., Gresty, M.A., Rothwell, J.C., Bronstein, A.M., 2009. Perceptual encoding of self-motion duration in human posterior parietal cortex. Annals of the New York Academy of Sciences 1164, 236–238. http://dx.doi.org/10.1111/j.1749-6632.2009.03772.x, 19645905.
Sprenger, A., Zils, E., Stritzke, G., Krüger, A., Rambold, H., Helmchen, C., 2006. Do predictive mechanisms improve the angular vestibulo-ocular reflex in vestibular neuritis? Audiology & Neuro-otology 11, 53–58. http://dx.doi.org/10.1159/000088926, 16224177.
Stephan, T., Deutschländer, A., Nolte, A., Schneider, E., Wiesmann, M., Brandt, T. et al, 2005. Functional MRI of galvanic vestibular stimulation with alternating currents at different frequencies. Neuroimage 26, 721–732. http://dx.doi.org/10.1016/j.neuroimage.2005.02.049, 15955481.
Strupp, M., Arbusow, V., Dieterich, M., Sautier, W., Brandt, T., 1998. Perceptual and oculomotor effects of neck muscle vibration in vestibular neuritis. Ipsilateral somatosensory substitution of vestibular function. Brain 121 (4), 677–685. http://dx.doi.org/10.1093/brain/121.4.677.
Suzuki, M., Kitano, H., Ito, R., Kitanishi, T., Yazawa, Y., Ogawa, T. et al, 2001. Cortical and subcortical vestibular response to caloric stimulation detected by functional magnetic resonance imaging. Brain Research. Cognitive Brain Research 12, 441–449. http://dx.doi.org/10.1016/S0926-6410(01)00080-5, 11689304.
Tschan, R., Wiltink, J., Best, C., Bense, S., Dieterich, M., Beutel, M.E. et al, 2008. Validation of the German version of the Vertigo Symptom Scale (VSS) in patients with organic or somatoform dizziness and healthy controls. Journal of Neurology 255, 1168–1175. http://dx.doi.org/10.1007/s00415-008-0863-1, 18481033.
Tschan, R., Wiltink, J., Best, C., Beutel, M., Dieterich, M., Eckhardt-Henn, A., 2010. Validation of the German version of the Vertigo Handicap Questionnaire (VHQ) in patients with vestibular vertigo syndromes or somatoform vertigo and dizziness. Psychotherapie, Psychosomatik, Medizinische Psychologie 60, e1–12.
Tzourio-Mazoyer, N., Landeau, B., Papathanassiou, D., Crivello, F., Etard, O., Delcroix, N. et al, 2002. Automated anatomical labeling of activations in SPM using a macroscopic anatomical parcellation of the MNI MRI single-subject brain. NeuroImage 15, 273–289. http://dx.doi.org/10.1006/nimg.2001.0978, 11771995.
van, den Heuvel M.P., Stam, C.J., Boersma, M., Hulshoff, Pol H.E., 2008. Small-world and scale-free organization of voxel-based resting-state functional connectivity in the human brain. Neuroimage 43, 528–539. http://dx.doi.org/10.1016/j.neuroimage.2008.08.010, 18786642.
Ventre-Dominey, J., Nighoghossian, N., Denise, P., 2003. Evidence for interacting cortical control of vestibular function and spatial representation in man. Neuropsychologia 41, 1884–1898. http://dx.doi.org/10.1016/S0028-3932(03)00126-X, 14572522.
Ventre, J., Faugier-Grimaud, S., 1986. Effects of posterior parietal lesions (area 7) on VOR in monkeys. Experimental Brain Research 62, 654–658, 3487465.
Vincent, J.L., Snyder, A.Z., Fox, M.D., Shannon, B.J., Andrews, J.R., Raichle, M.E. et al, 2006. Coherent spontaneous activity identifies a hippocampal–parietal memory network. Journal of Neurophysiology 96, 3517–3531. http://dx.doi.org/10.1152/jn.00048.2006, 16899645.
Zingler, V.C., Cnyrim, C., Jahn, K., Weintz, E., Fernbacher, J., Frenzel, C. et al, 2007. Causative factors and epidemiology of bilateral vestibulopathy in 255 patients. Annals of Neurology 61, 524–532. http://dx.doi.org/10.1002/ana.21105, 17393465.
Zingler, V.C., Weintz, E., Jahn, K., Mike, A., Huppert, D., Rettinger, N. et al, 2008. Follow-up of vestibular function in bilateral vestibulopathy. Journal of Neurology, Neurosurgery, and Psychiatry 79, 284–288. http://dx.doi.org/10.1136/jnnp.2007.122952, 17635972.
Zu, Eulenburg P., Baumgärtner, U., Treede, R.D., Dieterich, M., 2013. Interoceptive and multimodal functions of the operculo-insular cortex: tactile, nociceptive and vestibular representations. Neuroimage 83, 75–86, 23800791.
Zu, Eulenburg P., Caspers, S., Roski, C., Eickhoff, S.B., 2012. Meta-analytical definition and functional connectivity of the human vestibular cortex. NeuroImage 60, 162–169. http://dx.doi.org/10.1016/j.neuroimage.2011.12.032, 22209784.
Zu, Eulenburg P., Stoeter, P., Dieterich, M., 2010. Voxel-based morphometry depicts central compensation after vestibular neuritis. Annals of Neurology 68, 241–249. http://dx.doi.org/10.1002/ana.22063, 20695016.
Zuo, X.N., Ehmke, R., Mennes, M., Imperati, D., Castellanos, F.X., Sporns, O. et al, 2012. Network centrality in the human functional connectome. Cerebral Cortex (New York, N.Y.: 1991) 22, 1862–1875. http://dx.doi.org/10.1093/cercor/bhr269, 21968567.